Polymerization kinetics of wheat gluten upon thermosetting. A mechanistic model

Sandra Domenek, Marie Helene Morel, Joelle Bonicel, Stephane Guilbert

Polymerization Kinetics of Wheat Gluten upon Thermosetting. A Mechanistic Model

SANDRA DOMENEK, MARIE-HÉLÈNE MOREL,* JOËLLE BONICEL, AND STÉPHANE GUILBERT

Unité de Technologie des Céréales et des Agropolymères, ENSA.M-INRA, 2 Place Viala, F-34000 Montpellier, France

Size exclusion high-performance liquid chromatography analysis was carried out on wheat gluten−glycerol blends subjected to different heat treatments. The elution profiles were analyzed in order to follow the solubility loss of protein fractions with specific molecular size. Owing to the known biochemical changes involved during the heat denaturation of gluten, a mechanistic mathematical model was developed, which divided the protein denaturation into two distinct reaction steps: (i) reversible change in protein conformation and (ii) protein precipitation through disulfide bonding between initially SDS-soluble and SDS-insoluble reaction partners. Activation energies of gluten unfolding, refolding, and precipitation were calculated with the Arrhenius law to 53.9 kJ·mol^{-1}, 29.5 kJ·mol^{-1}, and 172 kJ·mol^{-1}, respectively. The rate of protein solubility loss decreased as the cross-linking reaction proceeded, which may be attributed to the formation of a three-dimensional network progressively hindering the reaction. The enhanced susceptibility to aggregation of large molecules was assigned to a risen reaction probability due to their higher number of cysteine residues and to the increased percentage of unfolded and thereby activated proteins as complete protein refolding seemed to be an anticooperative process.

KEYWORDS: Wheat gluten; polymerization; kinetic; mathematical model; heat treatment

INTRODUCTION

Temperature plays an important role in the processing of wheat gluten based products, as most texturization processes involve heat treatment of the material. On a molecular level, conformations of proteins, their polymeric state, and their interaction behavior are affected by temperature.

The application of texturization processes to wheat gluten, such as extrusion which is well studied in the field of food production (*1*−*7*), represents a real challenge to the production of biopolymers (*8*). To control the texturization processes and the properties of the final products, it is essential to get a better knowledge of the molecular changes in the proteins induced by shear on one hand and by temperature on the other.

This work focuses on the effect of temperature on gluten protein studied at a molecular scale and attempts to model the kinetics of gluten protein aggregation.

Gluten comprises protein monomers (gliadin) and polymers (glutenin) in roughly equal weight fractions. The molecular size (M_r) of gliadin polypeptides ranges from approximately 20000 up to approximately 80000 (ω-gliadin). Gliadin, except ω-gliadin, carries cysteine residues which are involved in intrachain disulfide bonds. Glutenin consists of discrete polypeptides (subunits), which are linked together by interchain disulfide bonds to form a high-molecular-weight polymer. The M_r of the subunits extends from about 36000 to 44000 for low M_r and from 60000 to 90000 for high M_r glutenin subunits. Glutenin polymers show a wide size distribution range, and their M_r may exceed several million (*9*, *10*). Flour glutenin is partly insoluble in most common solvents due to its huge size, even in the presence of denaturing agents such as sodium dodecyl sulfate (SDS). The wheat gluten solubility in SDS−phosphate buffer amounts to about 80−90% of the total protein mass. The wheat protein size distribution is usually studied by size exclusion high-performance liquid chromatography (SE-HPLC), which allows good resolution of gliadin monomers and glutenin polymers (*6*, *11*−*20*).

One of the most marked features of the heat-induced gluten denaturation is, e.g., the decrease of protein solubility in SDS−phosphate buffer. It has been evidenced in the literature that a rise of temperature causes protein unfolding which results in the exposition of hydrophobic protein zones. Protein aggregation may occur, in consequence, primarily due to hydrophobic interactions. The unfolded state facilitates thiol/disulfide interchange between exposed groups, which locks the protein into the denatured state due to the disulfide bond rearrangement (*5*, *6*, *11*, *18*).

The temperature dependency of gluten protein denaturation upon heating has been investigated by several groups. Their results are summarized in **Table 1**. The activation energy of the denaturation reaction, which can be calculated from the

Table 1. Activation Energy (E_a) of the Heat-Induced Denaturation of Wheat Gluten Protein Determined with Several Indicators

indicator	sample	water content (%)	E_a (kJ·mol^{-1})	ref
protein solubility	gluten	64.0–67.0	183	*21*
loaf volume	flour	8.0–19.9	270	*22*
	wheat	10.0	173	*23*
	wheat	20.0	164	*23*
	flour	21.6	137	*38*
	gluten	64.0–67.0	145	*21*

Arrhenius law, is a valuable tool to predict the progress of a reaction in dependency of temperature and to compare different studies since it is independent from time and temperature. However, it does not provide much insight into the reaction kinetics and the underlying molecular mechanisms.

In this work we aim to investigate kinetically the influence of temperature on gluten plasticized with glycerol in order to provide a comprehensive model of the heat-induced changes in gluten protein. To achieve our purpose, we investigated the effects of three heating temperatures (70, 82, and 94 °C) on the gluten protein solubility in SDS−phosphate buffer. To analyze the heat-induced changes in gluten proteins of specific M_r, we investigated the SDS−phosphate buffer extracts of the gluten samples with SE-HPLC. The continuous elution profiles were decomposed in individual protein peaks with the help of a Gaussian deconvolution fit. A mathematical model based on mechanistic reaction pathways was developed in order to calculate the solubility change of each protein species in SDS−phosphate buffer. The model sums up the current knowledge on the molecular events occurring during the heat-induced gluten solubility loss and the present results.

MATERIALS AND METHODS

Vital wheat gluten was provided by Amylum (Aalst, Belgium). Protein, starch, lipid, and ash amounted to respectively 76.5%, 11.8%, 5.0%, and 0.8% of dry mass. Moisture content was 7.2% (dry mass basis). Anhydrous glycerol was purchased from Fluka Chemie (Buchs, Switzerland) in p.a. quality. Chemicals for biochemical analysis of the samples were obtained from Sigma in p.a. quality.

Preparation of Heat-Treated Gluten−Glycerol Samples. Gluten (32.68 g) and glycerol (17.32 g) were hand-mixed in a mortar and rested for 20 min. The blend (3 g) was subsequently hand-molded to give a disk of 2 mm thickness and 4 cm diameter. The gluten/glycerol disk was sealed in a plastic bag under vacuum and incubated for increasing times in a water bath (E110, Lauda) regulated in temperature at 70, 82, or 94 °C. The bag was cooled in ice−water to stop the reaction, and the sample was stored at −28 °C. The most severe heat treatment was performed under a heating press (Techmo, Nazelles-Negron, France) at 120 °C for 35 min. The control sample (untreated), the sample treated at 120 °C, and three randomly chosen samples of the series at 82 °C were fabricated in triplicate.

Protein Size Distribution: SE-HPLC. The samples were analyzed according to the protocol of Redl et al. (*19*) with minor modifications. Ground samples (160 mg) were agitated for 80 min at 60 °C in 20 mL of 0.1 M sodium phosphate buffer (pH 6.9) containing 1% SDS (buffer A). The supernatant containing the SDS-soluble protein fraction (F_s) was collected after centrifugation (37000*g*, 30 min). The residue consisting of the SDS-insoluble protein fraction (F_i) was extracted with 5 mL of buffer A containing 20 mM dithioerythriol (DTE). The samples were agitated for 60 min at 60 °C and tip sonicated to bring total gluten protein in solution. The supernatant (500 μL) recovered after centrifugation (37000*g*, 30 min) was mixed with 500 μL of buffer A containing 40 mM iodoacetamide (IAM). IAM alkylated the thiol groups and prevented their subsequent oxidation. Both extracts (20 μL), F_s and F_i, were submitted to SE-HPLC fractionation.

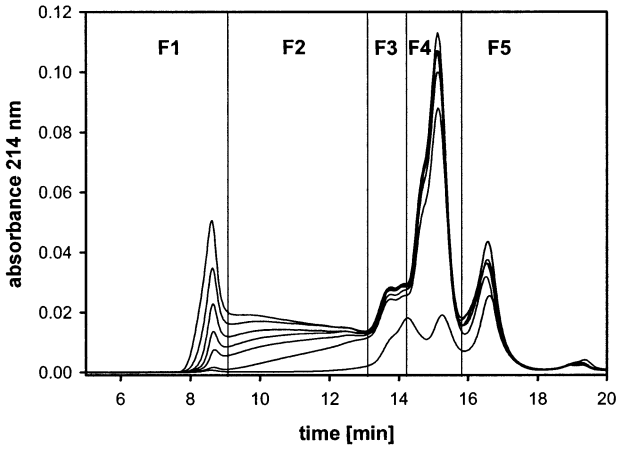

Figure 1. Changes of SE-HPLC profiles of the SDS-soluble protein fraction during heat treatment at 82 °C. Sample heat treatment (top to bottom): 0 (control sample, highest F1), 25, 120, 300, 420, 1140, and 1440 min at 82 °C. The lowest curve (no F1 or F2) corresponds to a sample treated for 35 min at 120 °C.

The fractionation was performed on a TSK-G 4000 SW XL (TosoHaas) analytical size exclusion column (7.5 × 300 mm) with a TSK 3000-SW XL (TosoHaas) guard column (7.5 × 75 mm). Columns were eluted at room temperature with 0.1 M sodium phosphate buffer (pH 6.9) containing 0.1% SDS. The flow rate was 0.7 mL·min^{-1}; proteins were detected at 214 nm. The apparent M_r of the proteins was estimated by calibrating the column with protein standards according to ref *12*. The elution profile of the supernatant was divided into five fractions (**Figure 1**). The lowest points on the valleys were used as cutoff points between the fractions. The area of each fraction was expressed in percent of total proteins, estimated from the sum of the total areas of the first and second extract (F_s and F_i) corrected for their different solid-to-solvent ratios. Fractions F1 and F2 include protein species having a M_r ranging from 1.5×10^6 to 150×10^3, which corresponds to the M_r of glutenin polymers (*24*). Proteins eluted in fractions F3 and F4 have a M_r ranging from 1×10^4 to 15×10^3 and can be assigned as gliadin (*13*, *24*). Fraction F5 consists mainly of metabolic proteins (albumins and globulins) and of α-gliadin. The coefficient of variation for the areas of the fractions, calculated from the triplicate experiments, did not exceed ±5%.

Chromatogram Analysis. The SE-HPLC elution profiles were adjusted according to the protein content of the samples which was determined by the Dumas method (NA 2000, Fisons instruments). A Gaussian deconvolution of the elution profile was performed using PeakFit v4 software (Jandel Scientific Software). The AutoFit Peaks III option was employed, which is based on a Fourier domain procedure deconvolving a Gaussian instrument response function from the raw data. The Gaussian fitting of the elution profile of the untreated gluten sample, which resulted in the detection of 27 peaks, served as template. The setting parameters employed for the untreated gluten were applied during the deconvolution of the other profiles. The peak number and position were fixed and the peak width variation was limited to less than 5%, whereas the peak height was fully adjustable. Fitting was performed with a least-squares minimization method in order to achieve a correlation coefficient higher than 0.999.

Calculation of the Model. The numeric calculation of the kinetic model was performed with Matlab 5.3.0 software (Mathworks Inc.). The differential equation system was solved with a variable order Adams−Bashforth−Moulton PECE solver (Matlab function "ode113") suitable for solving nonstiff differential equation systems (*25*). The reaction parameters were optimized by applying a least-squares minimization method (Matlab function "fmins") employing the Nelder−Mead simplex search algorithm (*26*, *27*).

RESULTS AND DISCUSSION

Solubility Changes of Heat-Treated Gluten Protein: Fitting with a First-Order Rate Law. The soluble protein fraction

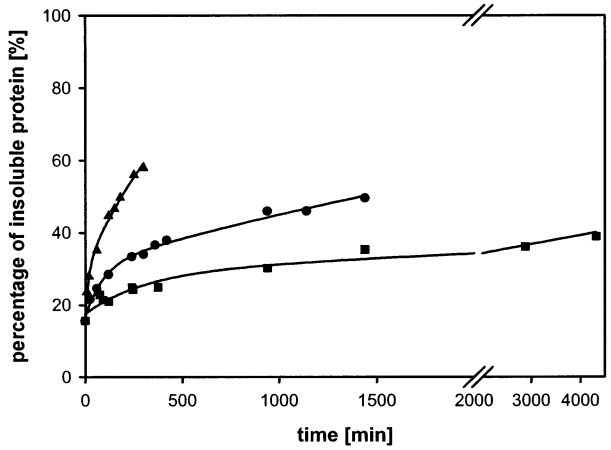

Figure 2. Increase of the percentage of the SDS-insoluble protein fraction due to heat treatment at different temperatures: 70 °C (■), 82 °C (●), and 94 °C (▲). Lines were calculated with a first-order exponential rate law considering two reaction constants.

of the heat-treated gluten/glycerol samples (at 70, 82, and 94 °C) was extracted using a sodium dodecyl sulfate (SDS)−phosphate buffer, which dissolved about 85% of the total protein mass of a native gluten sample. **Figure 1** shows the change in SE-HPLC profiles of the SDS-soluble gluten protein fraction (F_s) induced by a heat treatment at 82 °C. The elution profile is divided into five fractions. Fractions F1 and F2 correspond to glutenin polymers, fractions F3 and F4 can be assigned to gliadin proteins, and fraction F5 consists mainly of metabolic proteins (albumin and globulin) (*13*, *24*). The well-defined resolution between gliadin and glutenin polymer is ensured thanks to the strong disruptive power of SDS that suppresses electrostatic and/or hydrophobic interactions between the gluten proteins.

An overall decrease in the total SE-HPLC area can be observed upon heating, indicating a progressive protein solubility loss. The elution profile with the largest area corresponds to the control sample, which was not heat-treated. The curve displaying the smallest area shows the SE-HPLC profile of the control sample treated at 120 °C for 35 min. Due to its severity, this treatment is likely to give the maximum solubility loss under the employed experimental conditions. F1 and F2 completely disappeared after this severe heat treatment, while fractions F3−F5 remained soluble in significant amounts (F3, 22%; F4, 23%; and F5, 48%). The total solubility loss added up to 83% of the SDS-soluble gluten protein fraction. The change of elution profiles of the sample series at 82 °C showed that fractions F1 and F2 were more susceptible to heat treatment than fractions F3−F5. The solubility of the different protein fractions, F1−F5, dropped after 420 min of heat treatment at 82 °C to 13%, 61%, 93%, and 92%, respectively.

Strecker and co-workers (*28*) suggested that a step-grow polymerization mechanism accounted for the heat-induced aggregation of wheat gluten. The mechanism, which is appropriate for the radical-mediated synthesis of conventional polymers, describes the growth of polymer strands as a result of the sequential assembly of monomers. Step-growth polymerization typically results in a continuous shift of the size distribution profile toward larger species until their disappearance at the gel point (*29*). The change of the SE-HPLC profiles (**Figure 1**) did not support this hypothesis.

In contrast to the step-growth polymerization model, the solubility loss of glutenin polymers (fractions F1 and F2) seemed to proceed straightforward and all the more rapidly the larger the polymer size was (F1 before F2). We hypothesize that the direct conversion of soluble polymers to insoluble forms occurs through their covalent coupling with the already insoluble protein fraction. The cross-link is most likely a disulfide bond as the insoluble protein fraction was brought into solution after disulfide bond cleavage by DTE, as SDS buffer alone was not effective. Moreover, this is consistent with the well-known contribution of disulfide bonds to the heat-induced gluten polymerization (*11*).

In addition, we assume that the formation of a single disulfide bond between soluble and insoluble proteins is enough to ensure protein solubility loss. In consequence, the probability of coupling will rise with the polymer size because of the increasing number of cysteine residues per polymer chain.

To get further insight into the mechanism of gluten reactivity, we investigated the kinetics of the protein precipitation. **Figure 2** shows the increase of the SDS-insoluble protein fraction with time at different temperatures (70, 82, and 94 °C). The experimental data (plain symbols, **Figure 2**) could be described with a first-order rate law (continuous line), which considered two protein classes of different reactivity, as gliadin is known to be more stable to heat treatment than glutenin (*11*, *34*). Maximum protein solubility loss was set to 83.32% in accordance with the percentage of insoluble protein found in the heat-treated control sample (see above). A simple first-order rate law was already used by Pence et al. (*21*) and Becker and Sallans (*22*). It is commonly applied to polymerization (*30*, *31*) and to protein denaturation reactions (*32*, *33*).

The fitted rate constants showed that the temperature dependency of the reaction rate constants could be described with the Arrhenius law. The preliminary activation energy was calculated to 168 $kJ \cdot mol^{-1}$.

Lencki et al. (*32*, *33*) showed that, with appropriate assumptions with regard to the relative magnitudes of various reaction rates, many complex denaturation pathways can display apparent first-order behavior. The use of a first-order rate law, even if considering two protein classes, was still an oversimplified view of the gluten protein polymerization. The results presented in **Figure 1** showed evidence that glutenin (fractions F1 and F2) and gliadin (fractions F3 and F4) differed widely in their reactivity but also indicated that among glutenin polymers the larger proteins were more reactive.

Solubility Changes of Heat-Treated Gluten Protein: Fitting with a Mechanistic Model. To provide a more accurate interpretation of the observed rate constants, we separated the gluten denaturation in two different reaction steps: (i) reversible change in protein conformation and (ii) irreversible protein precipitation reaction through disulfide bonding.

The assumptions were coherent with the known biochemical changes during heat denaturation of gluten. Circular dichroism measurements on gliadin and low M_r glutenin subunits heated to 80 °C revealed that changes in the secondary protein structure were reversible, when proteins were cooled back to room temperature (*35*, *36*).

We describe the change in the protein conformation by

$$P_s \underset{k_{-1,d}}{\overset{k_{1,d}}{\rightleftharpoons}} P_s^* \qquad (1a)$$

where P_s and P_s^* represent a SDS-soluble protein before and after this transformation, respectively, and $k_{1,d}$ and $k_{-1,d}$ are the corresponding rate constants. As a first approximation, we neglect their possible dependence on the molecular weight of the protein. In particular, this should be applicable to very large proteins, such as the SDS-insoluble macropolymer P_i:

$$P_i \underset{k_{-1,d}}{\overset{k_{1,d}}{\rightleftharpoons}} P_i^* \quad (1b)$$

Unfolding of gluten protein resulted in the exposition of hydrophobic groups and cysteine residues, usually buried in the core of the molecule (*3*, *11*, *18*). We suppose the cross-linking reaction between SDS buffer soluble protein and the SDS-insoluble macropolymer is responsible for the protein precipitation. We write this irreversible process as

$$P_s^* + p_i^* \xrightarrow{k_{2,p}} p_a^* \quad (2)$$

where p_i^* (in contrast to P_i^*) denotes merely a section (of yet unknown size) of the protein P_i^*. For the following we quantify its mass $m_{p_i^*}$ with the help of the relation $m_{P_s^*} = \alpha m_{p_i^*}$, where α is a freely adjustable parameter. In the same way p_a^* stands for a section of the aggregated protein and $k_{2,p}$ is the corresponding rate constant. The protein precipitation may progress additionally through a P_s^*, becoming part of P_a^*, when reacting with it, i.e.

$$P_s^* \xrightarrow[P_a^*]{k_{3,p}} p_a^* \quad (3)$$

P_a^* will finally contain all of the insoluble protein mass. The reaction is driven by the rate constant $k_{3,p}$. The formation of covalent bonds between precipitated proteins may lock them into the denaturated state and thereby render complete refolding impossible. This hypothesis is supported by the observations of Schofield et al. (*11*).

In summary, the polymerization process of wheat gluten can be described by eqs 4−8, where the operator [ ] yields the actual mass of the given protein species (normalized with the total mass in the system). Equations 4−8 are in accordance with the mass balance given in eq 9:

$$\frac{d[P_s]}{dt} = -k_{1,d}[P_s] + k_{-1,d}[P_s^*] \quad (4)$$

$$\frac{d[P_i]}{dt} = -k_{1,d}[P_i] + k_{-1,d}[P_i^*] \quad (5)$$

$$\frac{d[P_s^*]}{dt} = k_{1,d}[P_s] - k_{-1,d}[P_s^*] - k_{2,p}\alpha[P_s^*][P_i^*] - k_{3,p}[P_s^*][P_a^*] \quad (6)$$

$$\frac{d[P_i^*]}{dt} = k_{1,d}[P_i] - k_{-1,d}[P_i^*] - k_{2,p}[P_s^*][P_i^*] \quad (7)$$

$$\frac{d[P_a^*]}{dt} = k_{2,p}(1+\alpha)[P_s^*][P_i^*] + k_{3,p}[P_s^*][P_a^*] \quad (8)$$

$$[P_t] = [P_s] + [P_s^*] + [P_i] + [P_i^*] + [P_a^*] + [P_{nr}] \quad (9)$$

where P_t denotes the total amount of proteins in the system and P_{nr} the percentage of nonreactive proteins. This percentage corresponds to the 16.68% of total gluten protein that remained soluble even after the severe heat treatment (120 °C for 35 min). Preliminary calculations showed that the temperature dependency of the reaction rate constants of protein denaturation ($k_{1,d}$, $k_{-1,d}$) and precipitation ($k_{2,p}$,$k_{3,p}$) followed the Arrhenius law:

$$k = Ae^{-E_a/RT} \quad (10)$$

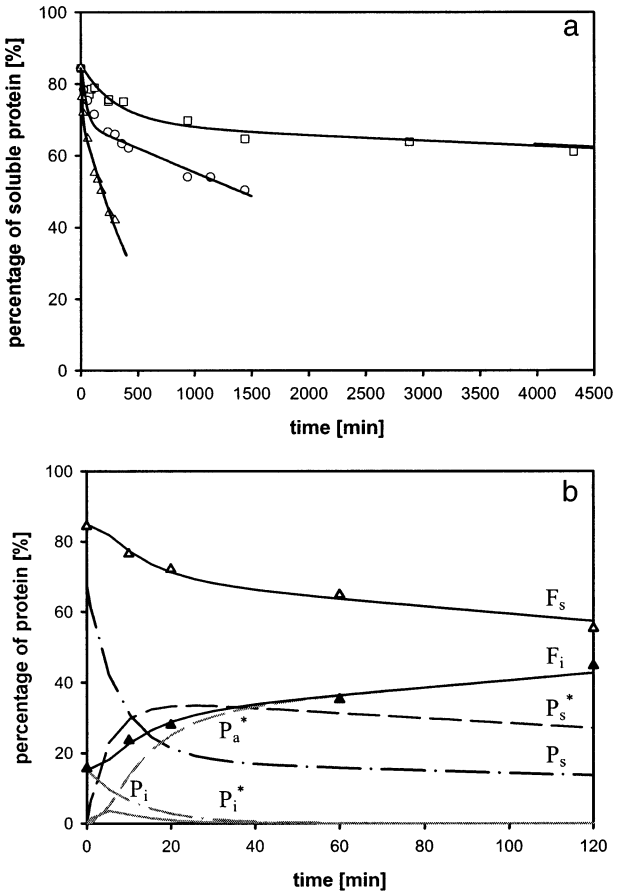

Figure 3. Fit of the mechanistic model (continuous line) to the experimental data of the gluten protein solubility loss in SDS buffer. Panel a shows the experimental data at different temperatures: 70 °C (□), 82 °C (○), and 94 °C (△). Panel b shows the zoom on the model calculation of the intermediates at 94 °C: native soluble protein P_s (–•–), native insoluble protein P_i (–•–), unfolded soluble protein P_s^* (– –), unfolded insoluble protein P_i^* (—), and aggregated protein P_a^* (– –).

Table 2. Fitted Model Parameters of the Heat-Induced Gluten Protein Precipitation[a]

constant	value	constant	value
$E_{a,D}$[b] (kJ·mol^{-1})	53.9	$E_{a,P}$[d] (kJ·mol^{-1})	172
$E_{a,R}$[c] (kJ·mol^{-1})	29.5	$A_{2,p}$[e] (min^{-1})	11.7×10^{22}
$A_{1,d}$[b] (min^{-1})	71.3×10^5	$A_{3,p}$[e] (min^{-1})	0.0985×10^{22}
$A_{-1,d}$[c] (min^{-1})	0.00998×10^5	R^2[f]	0.9910

[a] See text for details. [b] $E_{a,D}$ and $A_{1,d}$: activation energy and frequency factor of the unfolding reaction. [c] $E_{a,R}$ and $A_{-1,d}$: activation energy and frequency factor of the refolding reaction. [d] $E_{a,P}$: activation energy of both protein precipitation reactions. [e] $A_{2,p}$ and $A_{3,p}$: frequency factors of the precipitation reactions. [f] R^2: correlation coefficient between the experimental data and the model calculation ($n = 30$).

A is the Arrhenius frequency factor, E_a the activation energy, R the gas constant, and T the absolute reaction temperature.

Computing the rate constants directly with the Arrhenius law offers the advantage that the model constants can be optimized on the whole data set. **Figure 3a** shows that experimental and fitted data for F_s changes at different experimental temperatures (70, 82,, and 94 °C). The corresponding fitted parameters are given in **Table 2**. **Figure 3b** shows a zoom on the time curves of the different reactive species at 94 °C. We observe that the amount of unfolded SDS-soluble protein P_s^* reached its maximum after 20 min. The maximum coincided with the almost total disappearance of P_i and P_i^* and the slowing down

of F_s disappearance. The first reaction phase seemed to be governed by $k_{2,p}$ (P_i* reaction) and the second slower phase by $k_{3,p}$ (P_a* reaction). The large difference between rate constants $k_{2,p}$ and $k_{3,p}$ (frequency factors differing by 100; see **Table 2**) may be caused by two different effects. On one hand, gliadin is known to react more slowly than glutenin. The proportion between the two fractions would therefore shift with time toward an accumulation of gliadin in the soluble fraction. Consequently, rate constant $k_{2,p}$ would express the precipitation rate of glutenin and $k_{3,p}$ the precipitation rate of gliadin. This equals essentially the simplistic view adopted for our preliminary calculations and described in **Figure 2**. On the other hand, glutenin polymers (F1 and F2) summed up to about 29% of the total SDS buffer soluble protein mass, but F_s loss during the first reaction phase accounted only for 14% of the total soluble protein and coincided with the disappearance of P_i and P_i* (ca. 16% of the total protein mass). This finding led us to the hypothesis that the reaction slowdown came from the depletion of P_i*, which was more reactive than P_a*. The reactivity differences may be explained by the following considerations. The natively linear SDS-soluble polymers may be progressively incorporated into a three-dimensional insoluble network, which is building up. The protein network formation upon heating was indicated by rheological investigations on extruded and mixed gluten−glycerol samples (*7*, *19*). The increasing cross-link density within the network might decrease the reaction rate by hindering the molecular mobility. From this point of view, the use of two precipitation rate constants ($k_{2,p}$ and $k_{3,p}$) offered a simplified description of a continuous development.

The computed activation energy for the precipitation reactions 2 and 3 was 172 kJ·mol^{-1}. The value agreed well with previous studies, which are summarized in **Table 1**. The activation energies shown in **Table 1** were calculated with the help of simple first-order rate laws. Pence et al. (*21*) determined the activation energy directly from solubility loss experiments; the other teams measured the decrease in loaf volume of bread made from flour supplemented with heat-treated gluten. The different studies indicated that the reactivity of gluten was dependent on the water content of the sample (*18*, *22*−*34*). The good concordance found here with the values of other groups despite the use of glycerol as an alternative to water might indicate that glycerol did not to affect the energy of activation of the gluten polymerization upon heating.

The optimization of the model constants resulted in two different activation energies of protein unfolding and refolding (**Table 2**), which were roughly five to ten times lower than the E_a of precipitation. The energy barrier for unfolding was higher than the energy barrier for refolding, which reflects the fact that the native conformation of a protein corresponds to the conformation with the lowest energetic level. The equilibrium constant $K_{1,d}$ of reactions 1a and 1b can be calculated with the help of the relation:

$$K_{1,d} = \frac{k_{1,d}}{k_{-1,d}} \tag{11}$$

Using the van't Hoff equation

$$\frac{d \ln(K_{1,d})}{d(1/T)} = -\frac{\Delta_r H^{\theta}}{R} \tag{12}$$

we obtain the standard reaction enthalpy $\Delta_r H^{\theta}$, which equals to 24.4 kJ·mol^{-1}. Lullien-Pellerin et al. (*37*) investigated the conformational changes of γ46-gliadin under pressure. They calculated the free energy change of the conformational change of gliadin to be 38.4 kJ·mol^{-1}.

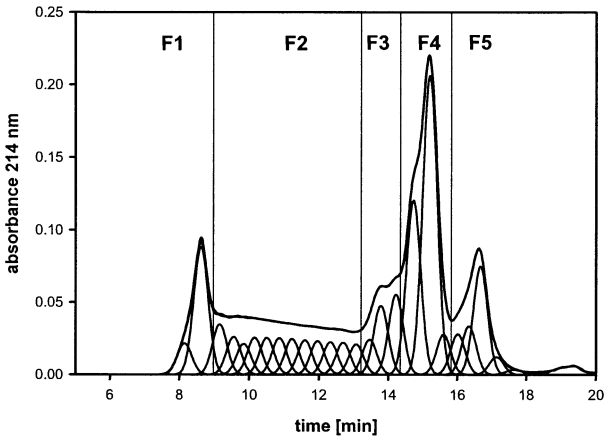

Figure 4. Gaussian deconvolution of the SE-HPLC profile of the SDS buffer soluble wheat gluten protein fraction of the control sample (no heat treatment).

The standard reaction enthalpy calculated with the present model has thus the same order of magnitude as the experimentally determined Gibbs energy.

Sensitivity of Gluten Protein Species to Heat Treatment: Effect of Molecular Size (M_r). The use of two rate constants ($k_{2,p}$ $k_{3,p}$) resulted in a simplified but accurate description of the presumed effect of the setup of an insoluble protein network. However, the changes in the SE-HPLC elution profiles (**Figure 1**) indicated that the precipitation rates varied even within fractions F1 and F2. To investigate the effect of the protein size on the reaction kinetics, a Gaussian deconvolution of the SE-HPLC profiles was performed. **Figure 4** shows the decomposition of the gluten control sample SE-HPLC elution profile into 27 individual protein species having molecular weights ranging from 1150000 to 3000. The protein solubility loss of each single peak was subsequently analyzed.

The solubility loss of gliadin monomers (F3 and F4; M_r 50000−38000−19000) can be fitted successfully with a first-order rate law. A striking exception was the gliadin monomer of M_r 74000, which showed no significant solubility loss even after 5 h at 94 °C. However, this finding was consistent with the known behavior of ω-gliadin (M_r 72000), which is claimed to be the only gluten protein that remains soluble even after severe heat treatments (*11*). Its heat stability is commonly attributed to its cysteine deficiency.

Protein peaks deconvolved in fraction F5 ($M_r \leq 16000$) showed steady solubility drop as well as transient increases. However, change of the total area of F5 could be modeled with a first-order rate law.

The protein species belonging to fractions F1 (M_r 1150000−843000) and F2 (M_r 676000−92000) displayed complex solubility drops, which could not be fitted without considering two levels of reactivity in each individual protein peak. The behavior is consistent with the main feature of the mechanistic model, which says that the deceleration of the precipitation rate due to steric hindrance caused by the concomitant network formation results in two apparent rate constants. The different rate constants may be attributed to the reactivity difference of P_i* and P_a*. The precipitation of gliadin monomers, which appears to be slower than the glutenin reaction, may essentially proceed through the reaction with P_a* in the later phase, as P_i* is already depleted. This may explain why first-order rate laws successfully model the solubility drops of gliadin.

Table 3. Fitted Model Parameters of the Heat-Induced Precipitation of Wheat Gluten Proteins of Specific M_r[a]

M_r	$A_{1,di}$ (min^{-1}) (×10^{-5})	$A_{-1,di}$ (min^{-1}) (×10^{-5})	$A_{2,p}$ (min^{-1}) (×10^{-22})	$A_{3,p}$ (min^{-1}) (×10^{-22})	$E_{a,D,i}$ (kJ·mol^{-1})	$E_{a,R,i}$ (kJ·mol^{-1})	R^2
1151069	80.5	0.0100	177	3.84	46.3	34.3	0.9906
1015636	55.1	0.00462	108	1.64	43.2	54.4	0.9669
842773	55.5	0.00727	70.3	2.92	46.9	37.0	0.9923
676309	59.8	0.00822	52.7	2.94	45.8	38.0	0.9948
553093	61.5	0.00748	35.0	2.67	45.2	32.9	0.9954
454051	75.6	0.0103	26.2	2.27	44.4	36.2	0.9955
372757	84.5	0.00988	18.7	1.85	46.8	34.6	0.9955
305808	82.4	0.0100	15.1	1.85	46.8	34.6	0.9955
250482	58.5	0.0145	14.7	1.62	48.6	28.6	0.9954
205109	59.2	0.0154	12.5	2.09	49.8	28.3	0.9952
168262	62.9	0.0165	13.7	1.74	51.0	27.6	0.9944
137719	58.2	0.159	12.4	2.33	52.2	27.6	0.9906
112994	57.5	0.0162	12.2	2.21	52.7	26.8	0.9792

[a] See text for details. [b] $E_{a,D,i}$ and $A_{1,di}$: activation energy and frequency factor of the unfolding reaction. [c] $E_{a,R,i}$ and $A_{-1,di}$: activation energy and frequency factor of the refolding reaction. [d] $A_{2,p}$ and $A_{3,p}$: frequency factors for the two precipitation reactions ($E_{a,D}$, see **Table 2**). [e] R^2: correlation coefficient between the experimental data and the model calculation ($n = 30$).

The mechanistic model was solved for each individual peak within fractions F1 and F2. The following suppositions were made. The precipitation activation energy of 172 kJ·mol^{-1} applies to all gluten proteins, which means that the rate of the disulfide-bonding reaction was independent for M_r. The rate constants of the protein unfolding ($k_{1,d}$ and $k_{-1,d}$, reaction 1b) represent an average value over all M_r, which can be applied to the unfolding reaction of the macropolymer. For the following, constants $k_{1,di}$ and $k_{-1,di}$ denote the unfolding and refolding rate constants of an individual soluble protein. The start ratio between F_s and F_i was set to 29/16, which equals the ratio between the SDS-soluble protein belonging to fractions F1 and F2 (28.82%) and F_i (15.64%). The assumption implies that (i) P_i* consumption results only from the reaction with glutenin polymers (fractions F1 and F2) and (ii) P_i* reacts randomly with glutenin polymers.

Figure 5 shows typical fitted time curves obtained for the different reacting species. The protein solubility loss (plain symbol) is described accurately for both protein peaks respectively from F1 and F2 (**Figure 5**). We observe an initial P_s* burst due to protein unfolding, so that the model curve corresponding to P_s* overlaps with the curve corresponding to F_s (**Figure 5a**). Then, P_s* reacted essentially with P_i* according to eq 2 until the P_a* concentration approximated that of P_i*. Subsequently, after the near depletion of P_i*, protein solubility loss slowed, being now governed by eq 3.

The model constants fitted for all of the peaks obtained from fractions F1 and F2 are given in **Table 3**. The percent of the denatured and thereby activated protein fraction F*can be calculated according to

$$F^* = 100 - \frac{100}{1 + K_{1,di}} \qquad (13)$$

where $K_{1,di}$ is the unfolding equilibrium constant of an individual protein. **Figure 6** shows the percentage of activated protein and the refolding rate constant versus their molecular weight. The percent of activated species increased gradually with protein size to 100% (calculated at 82 °C) above M_r 373000. This behavior was mainly caused by the drop of the refolding rate constant. The renaturation of large polymer seems to be an anticooperative process. The increased proportion of the activated forms of large polymers may thus contribute to their higher precipitation rates compared to smaller molecules.

The Arrhenius frequency factor $A_{2,p}$ appears to be exponentially related to the molecular weight of the polymeric chains.

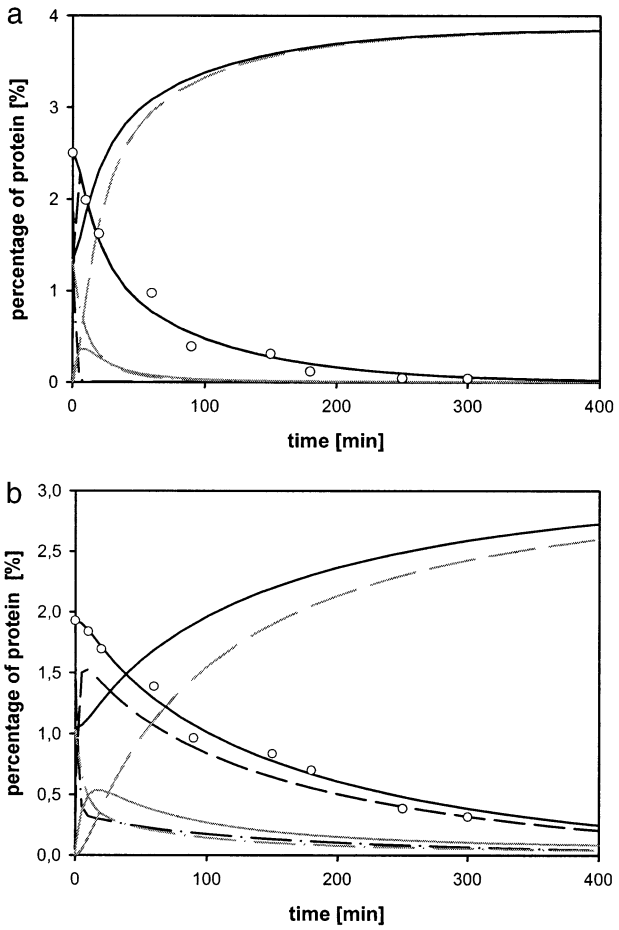

Figure 5. Fit of the mechanistic model (continuous line) to the solubility loss of the deconvolved protein species (○) at 94 °C. Panel a shows the solubility loss of the protein species M_r 842800 and panel b the solubility loss of the protein species M_r 250500. Lines correspond to the calculated intermediates: native soluble protein P_s (–·–), native insoluble protein P_i (–·–), unfolded soluble protein P_s* (– –), unfolded insoluble protein P_i* (—), and aggregated protein P_a* (– –).

Figure 7 shows the dependency of the precipitation Arrhenius factor on the molecular size of the proteins. The rise of the frequency factor expresses the enhanced probability of large molecules to react with insoluble partners (P_i* and P_a*). The hypothesis, assuming that the protein precipitation results from

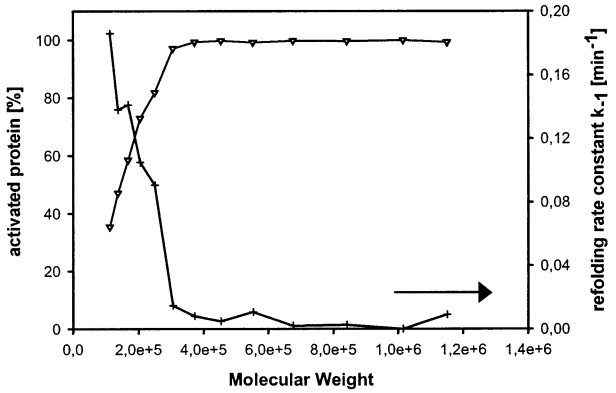

Figure 6. Dependency of the percentage of activated protein (▽, left scale) and the refolding constant k_{-1} (+, right scale) on the molecular weight of individual peaks at 82 °C.

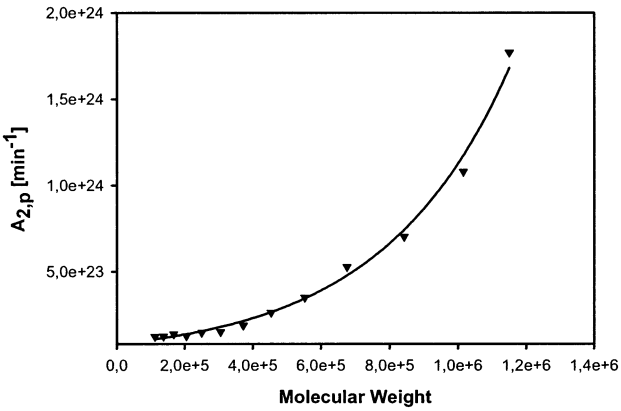

Figure 7. Dependency of the precipitation Arrhenius frequency factor $A_{2,p}$ (▼) on the molecular size.

the formation of a single disulfide bond between soluble and insoluble protein species, would thus be indirectly confirmed. Large polymers including more cysteine residues would present higher probability to cross-link with an insoluble partner. Both effects, higher percentage of activated species and higher reaction probability for the largest molecules, might provide a valuable explication for the reactivity differences within the glutenin fractions observed in **Figure 1**.

CONCLUSION

A mechanistic model that fits the precipitation of wheat gluten protein was established and proved valid for the temperature range investigated. Due to the known biochemical changes involved during heat denaturation of gluten, we proposed that protein aggregation would involve two steps: first, a reversible change in protein conformation and, second, a precipitation reaction through disulfide bonding. The slowdown of the precipitation rate with the progress of the reaction was assigned to steric hindrance resulting from the formation of a three-dimensional protein network in place of the linear native glutenin polymers.

The rise of the precipitation rates of SDS-soluble proteins with the increase of their molecular size supports the hypothesis that the protein solubility proceeds through a direct disulfide bonding between soluble and insoluble protein. The analysis of the reaction mechanism and its mathematical description may provide further insight in the formation of the gluten protein network upon thermosetting. Thereby, it could help to understand, at a molecular scale, the effects of temperature during gluten mixing and extrusion.

LITERATURE CITED

(1) Rebello, C.; Schaich, K. Extrusion chemistry of wheat flour proteins: II. Sulfhydryl-disulfide content and protein structural changes. *Cereal Chem.* **1999**, *76*, 756−763.

(2) Schaich, K.; Rebello, C. Extrusion chemistry of wheat flour proteins: I. Free radical formation. *Cereal Chem.* **1999**, *76*, 748−755.

(3) Li, M.; Lee, T. Effect of extrusion temperature on solubility and molecular weight distribution of wheat flour proteins. *J. Agric. Food Chem.* **1996**, *44*, 763−768.

(4) Li, M.; Lee, T. Effect of cysteine on the functional properties and microstructures of wheat flour extrudates. *J. Agric. Food Chem.* **1996**, *44*, 1871−1880.

(5) Li, M.; Lee, T.-C. Relationship of the extrusion temperature and the solubility and disulfide bond distribution of wheat proteins. *J. Agric. Food Chem.* **1997**, *45*, 2711−2717.

(6) Redl, A.; Morel, M.; Bonicel, J.; Vergnes, B.; Guilbert, S. Extrusion of wheat gluten plasticized by glycerol: Influence of process conditions on flow behavior, rheological properties and molecular size distribution. *Cereal Chem.* **1999**, *76*, 361−370.

(7) Redl, A.; Morel, M.-H.; Vergnes, B.; Guilbert, S. Rheological and biochemical approaches describing changes in molecular structure of gluten proteins during extrusion. *Wheat gluten* **2000**, 430−434.

(8) Cuq, B.; Gontard, N.; Guilbert, S. Proteins as agricultural polymers for packaging production. *Cereal Chem.* **1998**, *75*, 1−9.

(9) Wrigley, C. W. Giant proteins with flour power. *Nature* **1996**, *381*, 738−739.

(10) Southan, M.; MacRitchie, F. Molecular weight distribution of wheat proteins. *Cereal Chem.* **1999**, *76*, 827−836.

(11) Schofield, J.; Bottomley, R.; Timms, M.; Booth, M. The effect of heat on wheat gluten and the involvement of sulphydryl-disulphide interchange reactions. *J. Cereal Sci.* **1983**, *1*, 241−253.

(12) Dachkevitch, T.; Autran, J. Prediction of baking quality of bread wheats in breeding programs by size exclusion high performance liquid chromatography. *Cereal Chem.* **1989**, *66*, 448−456.

(13) Singh, N.; Donovan, G.; Batey, I.; MacRitchie, F. Use of sonication and size-exclusion high-performance liquid chromatography in the study of wheat flour proteins. I. Dissolution of total proteins in the absence of reducing agents. *Cereal Chem.* **1990**, *67*, 150−161.

(14) Singh, N.; Donovan, G.; Batey, I.; MacRitchie, F. Use of sonication and size-exclusion high-performance liquid chromatography in the study of wheat flour proteins. II. Relative quantity of glutenin as a measure of breadmaking quality. *Cereal Chem.* **1990**, *67*, 161−170.

(15) Gao, L.; Bushuk, W. Polymeric glutenin of wheat lines with varying number of high molecular weight glutenin subunits. *Cereal Chem.* **1993**, *70*, 475−480.

(16) Gupta, R.; Khan, K.; MacRitchie, F. Biochemical basis of flour properties in bread wheats. I. Effect of variation in quantity and size distribution of polymeric protein. *J. Cereal Sci.* **1993**, *18*, 23−41.

(17) Weegels, P.; Verhoek, J.; deGroot, A.; Hamer, R. Effects on gluten of heating at different moisture contents. I. Changes in functional properties. *J. Cereal Sci.* **1994**, *19*, 31−38.

(18) Weegels, P.; Verhoek, J.; deGroot, A.; Hamer, R. Effects on gluten of heating at different moisture contents. II. Changes in physico-chemical properties and secondary structure. *J. Cereal Sci.* **1994**, *19*, 39−47.

(19) Redl, A.; Morel, M.; Bonicel, J.; Guilbert, S.; Vergnes, B. Rheological properties of gluten plasticized with glycerol: dependence on temperature, glycerol content and mixing conditions. *Rheol. Acta* **1999**, *38*, 311−320.

(20) Morel, M.; Dehlon, P.; Autran, J.; Leygue, J.; Bar-L'Helgouac'h, C. Effects of temperature, sonication time, and power settings on size distribution and extractability of total wheat flour proteins as determined by size-exclusion high-performance liquid chromatography. *Cereal Chem.* **2000**, *77*, 685−691.
(21) Pence, J.; Mohammad, A.; Mecham, D. Heat denaturation of gluten. *Cereal Chem.* **1953**, *30*, 115−126.
(22) Becker, H.; Sallans, H. A study of the relation between time, temperature, moisture content, and loaf volume by the bromate formula in the heat treatment of wheat and flour. *Cereal Chem.* **1956**, *33*, 254−265.
(23) Schreiber, H.; Mühlbauer, W.; Wassermann, L.; Kuppinger, H. Reaktionskinetische Untersuchungen über den Einfluss der Trocknung auf die Qualität von Weizen. *Z. Lebensm.-Unters. -Forsch.* **1981**, *173*, 169−175.
(24) Kasarda, D.; Nimmo, C.; Kohler, G. Proteins and the amino acid composition of wheat fractions. In *Wheat. Chemistry and Technology*; Pomeranz, Y., Ed.; AACC: St. Paul, MN, 1988; pp 227−299.
(25) Shampine, L.; Gordon, M. *Computer solution of ordinary differential equations: the initial value problem*; Freeman: San Francisco, CA, 1975.
(26) Nelder, J.; Mead, R. A simplex method for function minimization. *Comput. J.* **1964**, *7*, 308−313.
(27) Dennis, J.; Woods, D. *New computing environments: Microcomputers in large-scale computing*; Wouk, A., Ed.; SIAM, 1987; pp 116−122.
(28) Strecker, T.; Cavalieri, R.; Zollars, R.; Pomeranz, Y. Polymerization and mechanical degradation kinetics of gluten and glutenin at extruder melt−section temperatures and shear rates. *J. Food Sci.* **1995**, *60*, 532−537.
(29) Matyjaszewski, K.; Gaynor, S.; Müller, A. Preparation of hyperbranched polyacrylates by atom transfer radical polymerization. 2. Kinetics and mechanism of chain growth for the self-condensing vinyl polymerization of 2-((2-bromopropionyl)oxy)-ethyl acrylate. *Macromolecules* **1997**, *30*, 7034−7041.
(30) Litvinenko, G.; Müller, A. General kinetic analysis and comparison of molecular weight distributions for various mechanisms of activity exchange in living polymerizations. *Macromolecules* **1997**, *30*, 1253−1266.
(31) Schmitt, B.; Müller, A. Anionic polymerization of (meth)acrylates in the presence of tetraalkylammonium halide-trialkyl aluminum complexes in toluene. 3. Kinetic investigations on primary acrylates. *Macromolecules* **2001**, *34*, 2115−2120.
(32) Lencki, R.; Arul, J.; Neufeld, R. Effect of subunit dissociation, denaturation, aggregation, coagulation, and decomposition on enzyme inactivation kinetics. I: First-order behavior. *Biotechnol. Bioeng.* **1992**, *40*, 1421−1426.
(33) Lencki, R.; Arul, J.; Neufeld, R. Effect of subunit dissociation, denaturation, aggregation, coagulation, and decomposition on enzyme inactivation kinetics. II: Biphasic and grace period behavior. *Biotechnol. Bioeng.* **1992**, *40*, 1427−1434.
(34) Weegels, P.; Hamer, R. Temperature-induced changes of wheat products. In *Interactions: The keys to cereal quality*; Hamer, R. J.; Hoseney, R. C., Eds.; AACC: St. Paul, MN, 1998; pp 95−130.
(35) Tatham, A.; Shewry, P. The conformation of wheat gluten proteins. The secondary structures and thermal stabilities of alpha-, beta-, gamma-, and omega-Gliadins. *J. Cereal Sci.* **1985**, *3*, 103−113.
(36) Tatham, A.; Field, J.; Smith, S.; Shewry, P. The conformations of wheat gluten proteins, II, aggregated gliadins and low molecular weight subunits of glutenin. *J. Cereal Sci.* **1987**, *5*, 203−214.
(37) Lullien-Pellerin, V.; Popineau, Y.; Meersman, F.; Morel, M.-H.; Heremans, K.; Lange, R.; Balny, C. Reversible changes of the wheat γ46 gliadin conformation submitted to high pressure and temperatures. *Eur. J. Biochem.* **2001**, *268*, 1−9.